



Unusual compressive plasticity of a centimeter-diameter Zr-based bulk metallic glass with high Zr content

Y.H. Li^{a,b}, W. Zhang^{a,c,*}, C. Dong^a, J.B. Qiang^{a,c}, K. Yubuta^c, A. Makino^c, A. Inoue^d

^a School of Materials Science and Engineering, Dalian University of Technology, Dalian 116024, PR China

^b Graduate school, Tohoku University, Sendai 980-8577, Japan

^c Institute for Materials Research, Tohoku University, Sendai 980-8577, Japan

^d Tohoku University, Sendai 980-8577, Japan

ARTICLE INFO

Article history:

Received 30 July 2009

Received in revised form 15 January 2010

Accepted 10 February 2010

Available online 18 February 2010

Keywords:

Bulk metallic glass
Mechanical property
Zr-based alloys
Compressive strain

ABSTRACT

The thermal stability, melting behavior, and glass-forming ability of $Zr_{70}Al_8Cu_{22-x}Ni_x$ ($x = 3-19$ at.%) metallic glasses were investigated. Fully glassy sample with largest critical diameter of 10 mm was obtained for alloy with $x = 8.5$ in the alloy series, which corresponds to a deep eutectic, largest supercooled liquid region, and largest γ value. Room temperature compression test revealed that the monolithic $Zr_{70}Al_8Cu_{13.5}Ni_{8.5}$ bulk metallic glass exhibits a high yield strength of 1570 MPa, a Young's modulus of 80 GPa, and a super large plastic strain more than 70%.

© 2010 Elsevier B.V. All rights reserved.

1. Introduction

Since the first report on the synthesis of a bulk metallic glass (BMG) in a special multi-component alloy system prepared by the copper mold casting method in 1989 [1], a number of BMGs have been found in various multi-component alloy systems and attracted much engineering interests [2–4]. The Zr-based BMGs are most expected to be used in engineering materials because they simultaneously have high glass-forming ability (GFA), high strength, good toughness, low cost and high corrosion resistance [5–7]. However, the absence of macroscopic plastic strain before fracture at the room temperature limited their applications [8].

Recently, a significant plastic deformation has been reported for Zr-based BMGs with high Zr contents (62.5–70 at.%) [9–11]. However, these Zr-based BMGs exhibit small critical size (d_c) for glass formation by copper mold casting, i.e., an inadequate GFA. Therefore, it is necessary to investigate the GFA and mechanical properties for the Zr-based alloys containing high Zr content, and to develop a BMG with high GFA (e.g., forming 1 cm diameter rods via copper mold casting) and good plasticity. In this paper, we investi-

gated the thermal stability, melting behavior, and GFA of Zr-based alloys with high Zr concentrations in $Zr_{70}Al_8Cu_{22-x}Ni_x$ series, and found that a near-eutectic $Zr_{70}Al_8Cu_{13.5}Ni_{8.5}$ alloy shows best GFA, and the full glassy samples with diameters up to 10 mm could be fabricated by copper mold casting. The BMG also exhibits a high yield strength of 1570 MPa and a super large plastic strain more than 70%. The underlying mechanism of the high GFA and unusual plastic deformation of the alloy is discussed.

2. Experimental procedure

The master ingots were prepared by arc melting the mixture of pure metals with purity of 99.9 mass% for Zr and 99.99 mass% for Al, Ni and Cu in a purified argon atmosphere. The ingots were melted repeatedly 4 times to make them chemical homogeneity. The pre-alloyed ingots were remelted and injected through quartz tube into copper cylindrical molds with diameters of 2–4 mm and a length of 40 mm under argon atmosphere. The tilt casting method was applied to prepare bulk glassy alloy rods of 5–12 mm in diameter and about 45 mm in length. Ribbon samples with a cross-section of 0.02 mm × 1.2 mm were prepared by melt spinning. The structure of the cast alloy rods was identified by X-ray diffraction (XRD) and transmission electron microscopy (TEM). The thermal stability associated with glass transition, supercooled liquid region and crystallization was examined by differential scanning calorimetry (DSC) at a heating rate of 0.67 K/s. The liquidus temperature and melting behavior were measured by differential thermal analyzer (DTA) at a heating rate of 0.33 K/s. Mechanical properties under a compressive applied load were measured by using an Instron testing machine. The specimen with a diameter of 2 mm and length of 4 mm was prepared for the compressive test and the strain rate was fixed as $5 \times 10^{-4} s^{-1}$. Young's modulus was measured by the strain gauge. The fracture morphology and deformation shear bands were examined by scanning electron microscopy (SEM).

* Corresponding author at: Institute for Materials Research, Tohoku University, Katahira 2-1-1, Aoba-ku, Sendai 980-8577, Japan. Tel.: +81 22 215 2470; fax: +81 22 215 2381.

E-mail address: wzhang@imr.tohoku.ac.jp (W. Zhang).

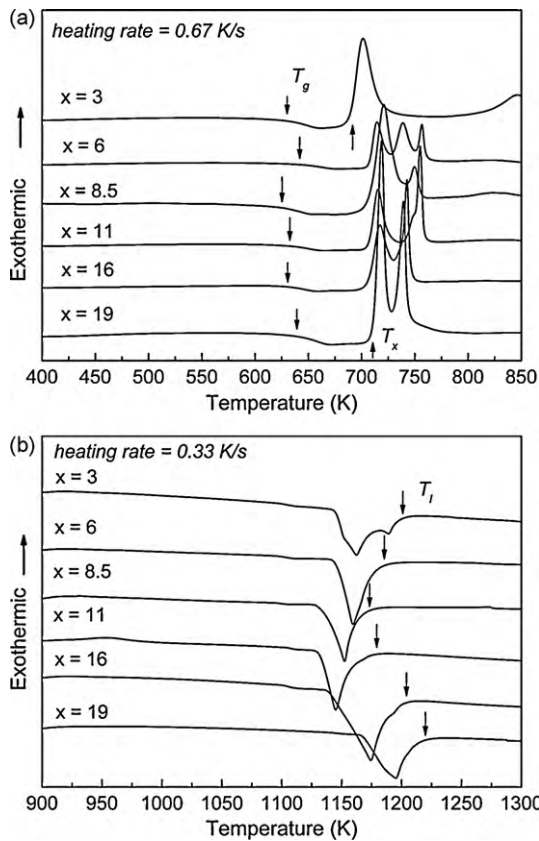


Fig. 1. DSC (a) and DTA (b) traces of $Zr_{70}Al_8Cu_{22-x}Ni_x$ ($x = 3-19$ at.%) glassy alloys.

3. Results and discussion

Fig. 1 shows DSC and DTA curves of $Zr_{70}Al_8Cu_{22-x}Ni_x$ ($x = 3-19$ at.%) metallic glasses. All the alloys show the sequent transition of glassy solid, i.e., an endothermic reaction due to glass transition, a large supercooled liquid region (ΔT_x defined by the difference between glass transition temperature T_g and crystallization temperature T_x) and then multistage exothermic peaks due to crystallization. The ΔT_x increases from 59 to 82 K with increasing x from 3 to 8.5, and then decreases to 70 K with further increasing x to 19. From DTA scans (Fig. 1(b)), the multiple events are observed during melting of the alloy with $x = 3$. The liquidus temperature (T_l) decreases with increasing x from 3 to 8.5, and the alloy with $x = 8.5$ exhibits the lowest T_l of 1171 K, and only a distinct endothermic peak. When the Ni content is further increased, the T_l rises and the endothermic peaks increase. These results indicate that the $Zr_{70}Al_8Cu_{13.5}Ni_{8.5}$ alloy is located near a deep eutectic in the quaternary alloys. From Table 1, it is noticed that although the alloy with $x = 8.5$ does not have a highest reduced glass transition temperature ($T_{rg} = T_g/T_l$), it shows largest ΔT_x and γ value ($\gamma = T_x/(T_g + T_l)$), indicating the higher GFA in the alloy series.

Fig. 2 shows the outer shapes and XRD patterns of the as-cast $Zr_{70}Al_8Cu_{13.5}Ni_{8.5}$ alloy rods. The alloy rods with diameters of 8

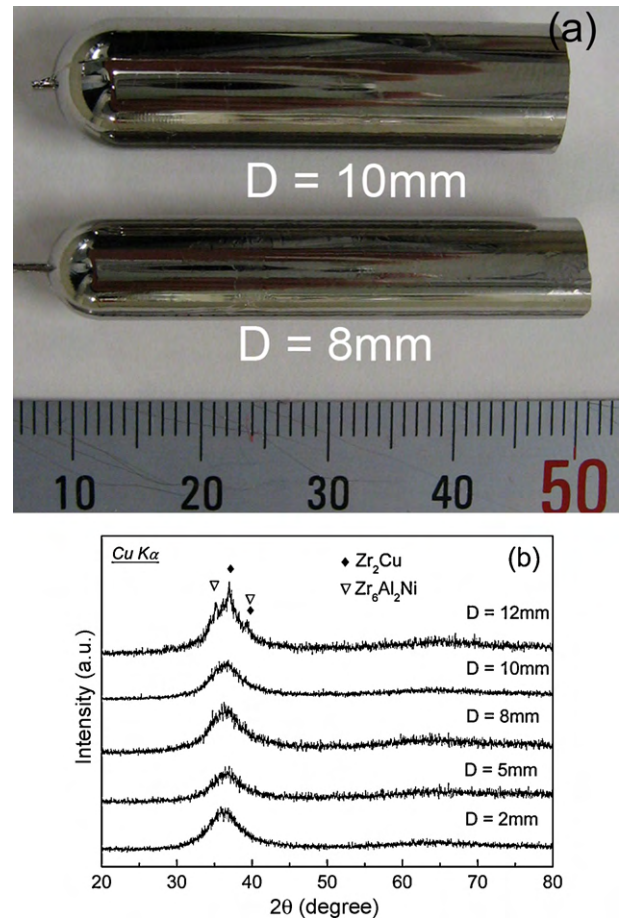


Fig. 2. Outer shapes (a) and XRD patterns (b) of as-cast $Zr_{70}Al_8Cu_{13.5}Ni_{8.5}$ alloy rods with different diameters.

and 10 mm exhibit very smooth surface and shiny luster. Neither ruggedness nor concave is observed over the whole outer surface (see Fig. 2(a)). These features indicate the absence of a distinct crystalline phase on the outer surface. The XRD patterns of the alloy rods with diameters of 2–10 mm only consist of broad peaks, and no diffraction peak corresponding to a crystalline phase is seen, indicating that a glassy phase is formed. A further increase in the rod diameter to 12 mm results in the precipitation of crystalline phases with $CuZr_2$ and Zr_6Al_2Ni . It is concluded that the critical sample diameter for formation of the glassy phase lies between 10 and 12 mm.

From Table 1, we also notice that the GFA of the alloys strongly depends on the Ni (or Cu) contents, and the best GFA is obtained for $Zr_{70}Al_8Cu_{13.5}Ni_{8.5}$, which is located at a deep eutectic (see Fig. 1(b)). The result agrees with the previous reports that the composition around the deep eutectic of multi-component alloys has a high GFA [6,12]. According to viewpoint of thermodynamics, the energy gap between liquid and solid states of the deep eutectic is smaller than that of non-eutectic, it makes quenching the liq-

Table 1

Summary of the thermal properties and the critical sample diameters of the $Zr_{70}Al_8Cu_{22-x}Ni_x$ ($x = 3-19$ at.%) alloys.

Compositions	T_g (K)	T_x (K)	ΔT_x	T_l	T_{rg}	γ	d_c (mm)
$Zr_{70}Al_8Cu_{19}Ni_3$	630	689	59	1200	0.525	0.377	<2
$Zr_{70}Al_8Cu_{16}Ni_6$	641	707	66	1179	0.544	0.388	6
$Zr_{70}Al_8Cu_{13.5}Ni_{8.5}$	625	707	82	1171	0.534	0.394	10
$Zr_{70}Al_8Cu_{11}Ni_{11}$	633	706	73	1175	0.539	0.390	8
$Zr_{70}Al_8Cu_6Ni_{16}$	631	705	74	1205	0.524	0.384	8
$Zr_{70}Al_8Cu_3Ni_{19}$	640	710	70	1220	0.525	0.382	<2

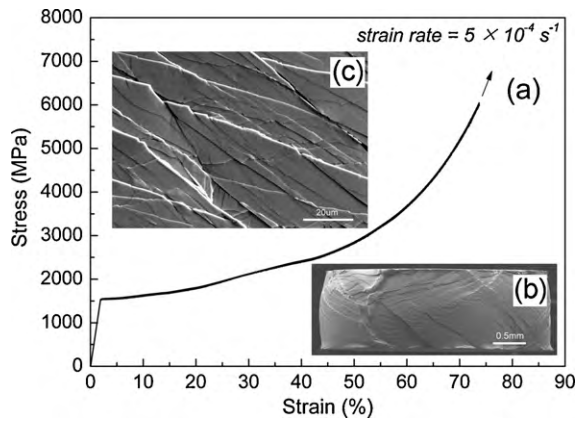


Fig. 3. Compressive stress–strain curve (a) and surface morphology (b and c) of $Zr_{70}Al_8Cu_{13.5}Ni_{8.5}$ glassy rod with a diameter of 2 mm.

uid to a glassy state easy before the formation of ordered crystals [13]. From aspect of kinetics, around eutectic, the multiple ordered phases compete with each other, and the crystallization of liquid requires simultaneous rearrangements of different kinds of atoms, which suppresses the kinetics of crystallization process, leading to the enhancement of the glass formation [14].

Fig. 3(a) shows the nominal compressive stress–strain curves of $Zr_{70}Al_8Cu_{13.5}Ni_{8.5}$ glassy rods with a diameter of 2 mm experienced 72% plastic strain. It can be seen that under compressive loading, the glassy alloy exhibits an initial elastic deformation behavior with an elastic strain about 1.9%, and then begins to yield at 1570 MPa, followed by significant plastic deformation more than 70% without fracture (see Fig. 3(b) of figure insert). The young's modulus is about 80 GPa. According to the calculated true stress–true strain curve, the true stress keeps nearly constant about 1.5 GPa without work-hardening. Fig. 3(b) shows the shape and outer morphology of a sample after compression test, and Fig. 3(c) is a magnified surface SEM image of the sample. It can be found that the dense multiple shear bands were formed all over the rod. The distribution of shear bands reveals that the propagation of crossed shear bands was hindered and new shear bands were initiated during the further strain, namely, the multi-stages shear bands were produced during the whole compression test, which results in a large compressive plasticity.

Since large compressive deformation has been reported for Zr-based BMGs, many factors have been developed to explain the mechanisms, such as nanocrystallizations [15–17], presenting soft/hard zones [9], high Poisson's ratio [18] and excessive free volumes [19]. Our experimental results obtained from detailed TEM analysis of the $Zr_{70}Al_8Cu_{13.5}Ni_{8.5}$ BMG have ruled out the presence of soft/hard zones. The high-resolution transmission electron microscopy (HRTEM) image (Fig. 4) confirms the absence of any nanocrystalline phase. The selected-area electron diffraction pattern also consists of only halo rings, indicating a purely glassy structure. As for Poisson's ratio factor, from the compositional dependence of Poisson's ratio for Zr–Ni–Cu–Al BMGs [11], it can be estimated that the eutectic $Zr_{70}Al_8Cu_{13.5}Ni_{8.5}$ alloy has a smaller Poisson's ratio as compared with a hypoeutectic BMG which has a high compressive ductility reported in Ref. [11]. The above results reveal that the large plastic deformation of the alloy is not controlled by factor of nanocrystallizations, soft/hard zones or Poisson's ratio.

It is widely recognized that the plastic deformation in BMGs can be largely enhanced by introducing interior heterogeneity, which can facilitate the initiation, bifurcation and intersection of shear bands. It is reported that the free volume can act as the beneficial site to initiate and bifurcate the shear bands, leading to enhance-

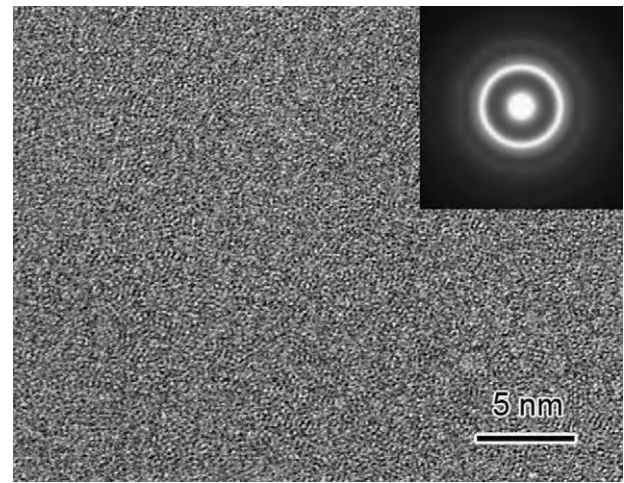


Fig. 4. High-resolution transmission electron micrograph and selected-area electron diffraction pattern of $Zr_{70}Al_8Cu_{13.5}Ni_{8.5}$ rod with a diameter of 2 mm.

ment in plasticity of BMGs [20]. Xie et al. [21] also confirmed that there is a qualitative correlation between the amount of free volume and the plasticity in a Zr-based BMG. In addition, it has been revealed that the free volume is always located near Zr atoms in the Zr-based BMGs [19,22]. Therefore, it can be presumed that the present alloy with a high Zr concentration of 70 at.% contains more free volume, resulting in a large compressive plasticity.

4. Summary

With the aim of developing a new Zr-based BMGs with high GFA and good plasticity, we examined the thermal stability, melting behavior, GFA and mechanical properties of Zr-based alloys with high Zr content of 70 at.% in $Zr_{70}Al_8Cu_{22-x}Ni_x$ ($x=3-19$ at.%). The best GFA is obtained for the eutectic alloy with $x=8.5$ corresponding to the largest ΔT_x of 82 K and γ value of 0.394, and the full glassy sample diameters up to 10 mm are formed by copper mold casting. In addition to its high GFA and high stabilization of supercooled liquid, this BMG exhibits high yield strength of 1570 MPa and super large compressive plastic strain more than 70%. The GFA obtained in this paper is the highest of all monolithic BMGs with significant plastic deformation. The combination of high GFA, large ΔT_x , high yield strength with a remarkable plasticity gives the new BMG excellent promise for both scientific and engineering applications.

Acknowledgments

This work was financially supported by Research and Development Project on Advanced Metallic Glasses, Inorganic Materials and Joining Technology from the Ministry of Education, Science, Sports, and Culture of Japan.

References

- [1] A. Inoue, T. Zhang, T. Masumoto, *Mater. Trans.* 30 (1989) 965.
- [2] A. Inoue, W. Zhang, T. Zhang, K. Kurosaka, *Acta Mater.* 49 (2001) 2645.
- [3] H. Ma, L.L. Shi, J. Xu, Y. Li, E. Ma, *Appl. Phys. Lett.* 87 (2005) 181915.
- [4] A. Peker, W.L. Johnson, *Appl. Phys. Lett.* 63 (1993) 2342.
- [5] A. Inoue, T. Zhang, Y.H. Kim, *Mater. Trans.* 38 (1997) 749.
- [6] Q.S. Zhang, W. Zhang, X.M. Wang, Y. Yokoyama, K. Yubuta, A. Inoue, *Mater. Trans.* 49 (2008) 2141.
- [7] A. Inoue, T. Zhang, *Mater. Trans.* 37 (1996) 185.
- [8] Z.F. Zhang, J. Eckert, L. Schultz, *Acta Mater.* 51 (2003) 1167.
- [9] Y.H. Liu, G. Wang, R.J. Wang, D.Q. Zhao, M.X. Pang, W.H. Wang, *Science* 315 (2007) 1385.
- [10] L. Zhang, Y.Q. Cheng, A.J. Cao, J. Xu, E. Ma, *Acta Mater.* 57 (2009) 1154.
- [11] Y. Yokoyama, K. Fujita, A.R. Yavari, A. Inoue, *Philos. Mag. Lett.* 89 (2009) 322.
- [12] W.L. Johnson, *Mater. Sci. Forum* 225–227 (1996) 35.

- [13] W.L. Johnson, JOM 54 (2002) 40.
- [14] D.H. Xu, G. Duan, W.L. Johnson, Phys. Rev. Lett. 92 (2004) 245504.
- [15] A. Inoue, W. Zhang, T. Tsurui, A.R. Yavari, A.L. Greer, Philos. Mag. Lett. 85 (2005) 221.
- [16] M. Chen, A. Inoue, W. Zhang, T. Sakurai, Phys. Rev. Lett. 96 (2006) 245502.
- [17] J.B. Qiang, W. Zhang, G.Q. Xie, A. Inoue, Appl. Phys. Lett. 90 (2007) 231907.
- [18] J. Schroers, W.L. Johnson, Phys. Rev. Lett. 93 (2004) 255506.
- [19] K. Mondal, T. Ohkubo, T. Toyama, Y. Nagai, M. Hasegawa, K. Hono, Acta Mater. 56 (2008) 5329.
- [20] L.Y. Chen, A.D. Setyawan, H. Kato, A. Inoue, G.Q. Zhang, J. Saida, X.D. Wang, Q.P. Cao, J.Z. Jiang, Scripta Mater. 59 (2008) 75.
- [21] S.H. Xie, X.R. Zeng, H.X. Qian, J. Alloys Compd. 480 (2009) L37.
- [22] T. Yano, Y. Yorikado, Y. Akeno, F. Hori, Y. Yokoyama, A. Iwase, A. Inoue, T.J. Konno, Mater. Trans. 46 (2005) 2886.